

CREEP TESTING OF A TIMBER LATTICE FRAME USING IMAGE RECOGNITION

Nicolas Giron¹, Hideyuki Nasu²

ABSTRACT: A one year creep testing for an architectural project was conducted for a 8650mm span timber lattice frame. In parallel of the standard measurement with dial gauges, three cameras were set and 400 pictures were taken on a regular base for the full year. To process the picture data, an image recognition program was used. The displacement of each node of the lattice frame was extracted and the central deflection of the frame was evaluated. The deflection measured by dial gauge and the one estimated by image recognition were compared and a very good accordance was observed. In addition to the central deflection, deformation and stress of each member of the lattice frame can be estimated, allowing to understand the global and the detailed behaviour of the frame. Applications of the proposed method are presented.

KEYWORDS: Creep testing, Image recognition, Structural analysis

1 INTRODUCTION

As timber is a viscoelastic material, creep amplification, which refers to amplification of elastic deflection over time, is an important factor to consider when designing a timber structure. For a single structural element, the range of the amplification is well documented for various periods of time and types of loading [1]. However, for a composite structure like the lattice frame presented below, accurately evaluating the expected amplification is difficult due to factors such as connections and the mix of loading types. For non-conventional types of structure with long-term deflection that may be critical, creep testing is frequently undertaken.

While creep testing a large structure is costly and time-consuming, generally only a few measurement devices are used, mainly to estimate the central deflection, leading to an understanding of the global behaviour of the structure but not the behaviour of each element.

In 2018, a creep testing using standard measurement devices was conducted for a full year. At that time, it was expected that in image recognition algorithms would be improved and become a powerful tool to enhance the results of such a testing. Therefore, distinctive marks, hereafter templates, were placed on the node of the lattice frame in anticipation of future research.

This article proposes a method using image recognition to estimate the creep amplification factor, along with other meaningful structural characteristics. Without installing any recording devices like dial gauges or strain gauges, the complete behaviour of a structure can be recorded using pictures taken by a standard camera (in this study, NIKON COOLPIX W300 with 16.05 million effective

pixels and a 1/2.3" CMOS image sensor)) and then analysed using an image recognition program.

The central deflection estimated through this proposed method shows good agreement with the measurement of the dial gauge. Additionally, the displacement and rotation of all the nodes, and the evolution of the length of each element of the lattice frame were estimated. While there are issues with accuracy and points to be improved, the authors believe that promising results were obtained, even if the testing that was planned for standard measurement method with no particular attention given to the proposed method.

A roof composed of frames similar to the tested lattice frame has been in service since four years in an elementary school in Japan (Figure 1), and to this day, the structural behaviour of the frames is within the design range.

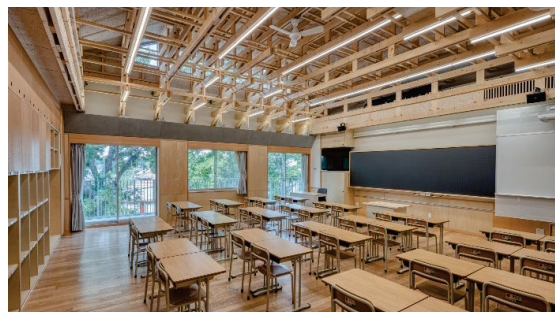


Figure 1: Classroom of the Seijogakuen Elementary school with lattice framed roof form of superimposed lumber and joined by wood screws and LVL gussets

¹ Nicolas Giron, NIKKEN SEKKEI LTD, (Engineering Department, Structural Design Section, 2-18-3 Iidabashi, Chiyoda-ku, Tokyo) Japan, giron.nicolas@nikken.jp

² Hideyuki Nasu, Nippon Institute of Technology, (4-1 Gakuendai, Miyashiro, Minamisaitama-gun, Saitama) Japan, hideyuki.nasu@nit.ac.jp

2 CREEP TESTING SETUP AND RESULTS

2.1 TESTED FRAME OUTLINE

A lattice frame system composed of superimposed dimension lumber (38x140 SPF) and laminated veneer lumber (LVL) gussets was tested. Lumbers are arranged on a grid with horizontal spans of 910mm and vertical spans of 400mm. The frame includes horizontal, vertical and diagonal elements. The frame consists of three layers with one vertical lumber in the centre between two horizontal or diagonal lumbers, giving the frame a total thickness of 114mm. When lumbers from more than two directions meet at one point, 38mm thick LVL gussets are inserted, as shown in Figure 2. The lumbers are connected using wood screws as a double shear connection. The screw length is 110mm with a thread length of 40mm, and the screw material is carbon steel wire for cold heading and cold forging (SWCH) respecting JIS G3507-2 regulation. Ruspert anti-corrosion treatment is applied. The lattice frame spans over 8.645m with a rise of 2m and a minimal depth of 400mm. Further details can be found in [2].

2.2 TESTING SETUP

Two frames were placed side by side in a hangar and connected at roof level by plywood. They were loaded with steel rebar for an entire year. Each frame was equipped with 3 dial gauges, as in Figure 3. In addition to the dial gauges, four cameras were placed (Cameras 1, 2, 3: NIKON COOLPIX W300, Camera 4: NIKON Keymission 170 (wide angle)). At each node of the frame, a template was placed (Figure 6) to facilitate the image recognition process. The frames were loaded using a total of 900 pieces of steel rebar, resulting in a total load of total load of 53kN, including the self-weight of the frames and the additional elements used to connect them. The total load corresponds to twice the expected long-term dead load considered in the design.

The testing began on August 27th, 2018, and ended one year later. The dial gauge data were collected every 10 minutes. During the first hour, pictures were taken every 10 minutes. Afterwards, picture were taken every hour until the next day, every 3 hours until the third day, every 6 hours until the fourth day, every 12 hours until the fifth day. Then, pictures were taken once a day during the first month and twice a week until the end of the testing for Cameras 1 to 3. For Camera 4, pictures were taken twice a week for 3 months.

2.3 RESULTS

The initial elastic deflection is approximately 17.82mm. The maximum deflections recorded after 1, 6 and 12 months are respectively 22.81mm (1.28 times), 27.29mm (1.53 times) and 33.08mm (1.86 times), respectively. The power law creep equation is used to evaluate the creep amplification coefficient at 50 years. The approximation of the power law equation parameters with the data recorded during one year yielded a 50-years deflection about 49mm and a creep amplification factor of 2.8. The results are presented in Figure 5.

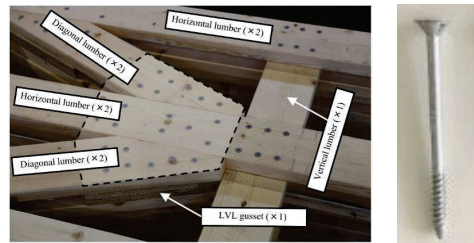


Figure 2: Left: LVL gusset connection, Right: wood screw

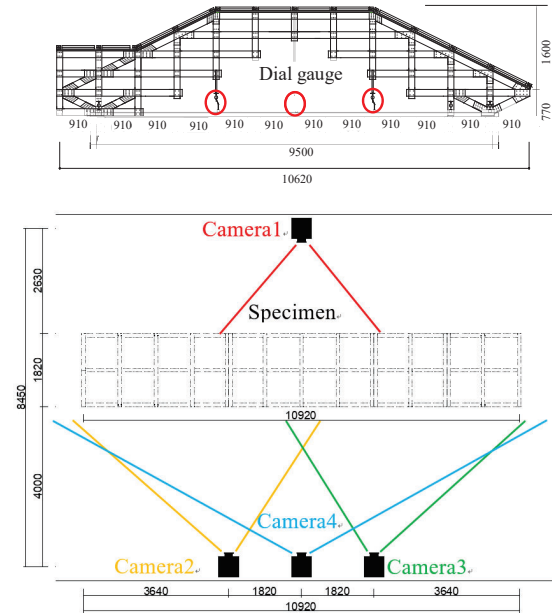


Figure 3: Top: Frame elevation, Bottom: Camera range

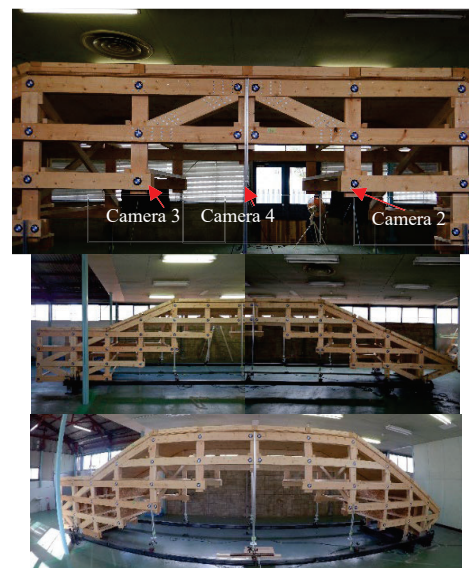


Figure 4: View from each Camera from 1 to 4

3 IMAGE RECOGNITION PROCEDURE

3.1 METHODOLOGY

The proposed method has been applied to the pictures from Camera 2 and Camera 3. The pictures from Camera 4 have large distortions due to the wide-angle lens and were not analysed this time. However, with an appropriate algorithm and some calibrations, it is possible to restore the true angles and geometry, allowing for the processing of the pictures in the same way.

The data are processed with a Python program using the OpenCV library for image recognition. The “matchTemplate” function is used, and results are calculated based on the normalized correlation coefficient. This function assigns a score between 0 and 1 to each pixel of the picture based on the resemblance between a given template and the corresponding picture area. For a single node, many matches are returned, and therefore, a filtering procedure is required to assign a unique coordinate to a node, as shown in Figure 7. The procedure is as follows:

In the first step, the images from Camera 2 and Camera 3 are combined to form a picture of the whole frame. The four marks of the overlapping area are used to determine the differences in scale and angular rotation of the two pictures, along with the coordinates where the images can be stitched. The two pictures are accordingly rotated, scaled and stitched, as shown in Figure 8.

In the second step, two areas of the pictures that are likely to be unchanged during the test process are chosen. Using the image recognition of the first step, all the pictures are scaled, rotated, resized and aligned to a common base with the same origin and axis from a reference picture, as shown in Figure 9. This allows the location of the marks in each picture to be compared, and the location variations correspond to the displacement of the frame.

In the third step, each node of the first picture is copied and rotated from -2.00 to 2.00 degrees with 0.01 degree intervals. The resulting images are saved as new templates for the next step, as shown in Figure 10.

In the fourth and last step, the original template is used to locate all the nodes. Then each node is compared with its dedicated template from -2.00 ~ 2.00 degrees from the first picture, and the template with the best matching is assumed to be the variation of the angle since the beginning of the testing. This process is detailed in the next section. In addition to the node marks, the three anchors of the frame to the ground are also located. Data is stored in an Excel sheet with coordinates and rotation angle of each node and the date of the picture. Also, the original pictures are edited with the located nodes, their number, and rotation angle, as shown in Figure 11.

The data is then available to be processed for structural analysis. The length of a known element is used to calibrate the pixel size, allowing the coordinates of each node to be calculated in millimetres.

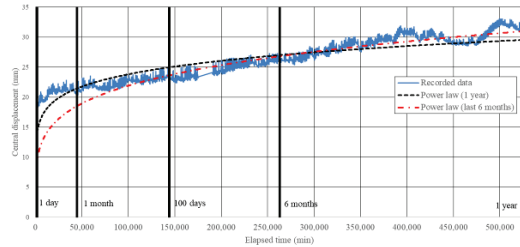


Figure 5: Creep testing records and power law approximations

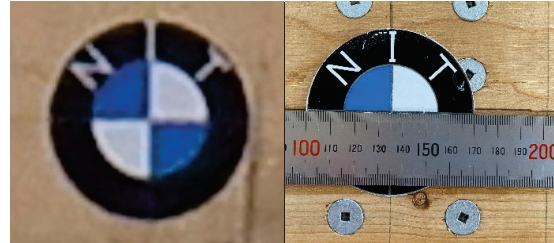


Figure 6: Left: Mark placed at each node with real picture resolution, Right: Size of the mark

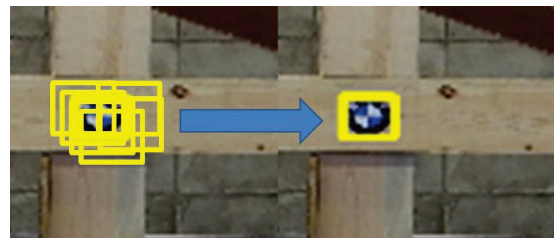


Figure 7: Results from the matching procedure before (left) and after filtering (right)



Figure 8: Step 1, pictures from Camera 2 and Camera 3 are rotated, scaled and stitched using the four centre marks



Figure 9: Step 2, reference picture on the left is used as a base to rotate, scale and align other pictures

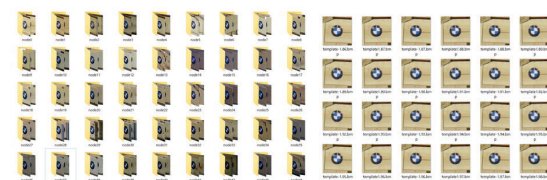


Figure 10: Step 3, for each node templates are created (left) with rotation from -2.00 to 2.00 degrees (right)

3.2 ROTATION ANGLE

To identify the variations in the rotation angle of a mark, the mark is compared to templates of various angles and the best match is chosen. Initially, a common template was planned for all the nodes, but during the evaluation process, issues arose.

Testing was conducted with digital data and real pictures with various backgrounds using the layout and rotation angles in Figure 12. Accurate results were obtained for digital data, but for real pictures, noise from the background and picture distortion had a significant impact, as seen in Figure 13. To reduce the noise, two options were considered: making the template as small as possible to remove the background and keep only the mark, or using a different template for each node to include the background into the identification process. The latter option was chosen because reducing the mark of the creep testing which is already small (55x55 pixels), would also reduce the minimum resolution available, while using a local template would allow for a larger template size 135x135 pixels that includes the background, improving resolution. Additionally, when limited to a located area, the impact of image distortion in the templates and pictures is approximately the same, mitigating its impact on the identification process.

For the digital testing, the results showed a continuous distribution with an error of +/- 0.02 degree for a 150x150 template, as shown in Figure 14. For the full scale creep testing, a resolution of around $2 \times 0.02 \times 150 / 55 = 0.11$ degrees is expected. However, with real pictures, the results included some noise, making it difficult to determine whether the best result is due to noise or is the true maximum. Results are expected to have a continuous bell shape distribution, and therefore, are approximated with a curve obtained with Savitzky-Golay filter, as in shown Figure 15.



Figure 11: Step 4, each node is assigned a unique number and rotation angle. Coordinates are saved in an Excel file

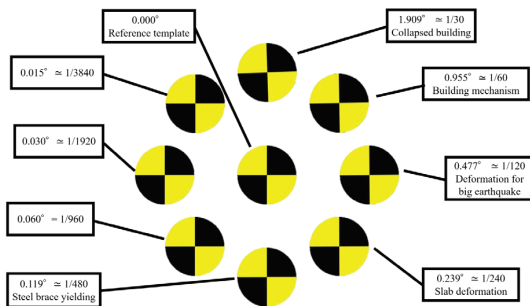


Figure 12: Rotation angle confirmation testing layout and angle

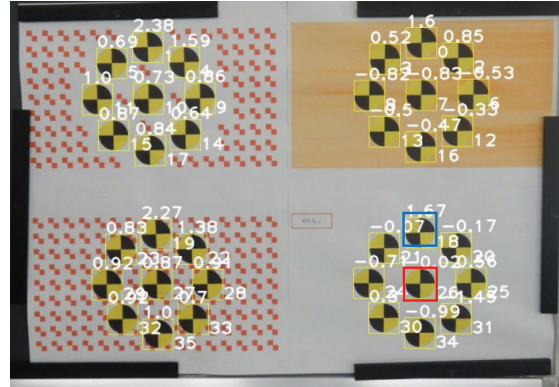


Figure 13: Results for different background with real picture (template in red)

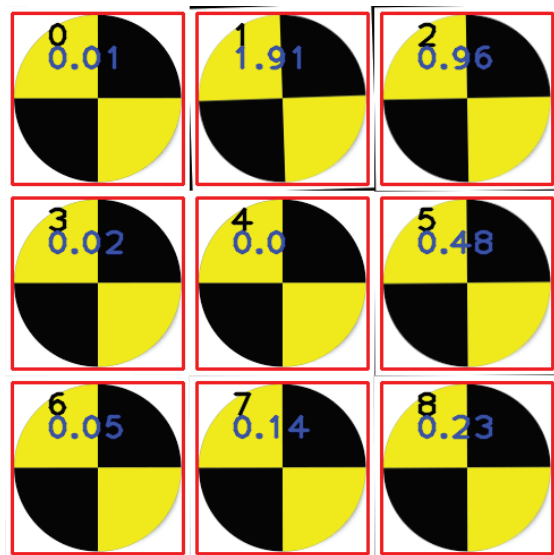


Figure 14: Red template from Figure 13 is rotated and placed as in Figure 12.

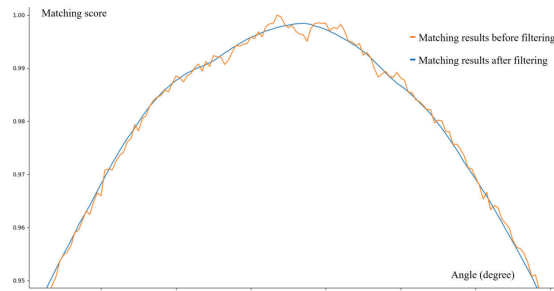


Figure 15: Scoring for each angle for the blue template of Figure 13

4 STRUCTURAL ANALYSIS

4.1 FRAME DISPLACEMENT

By estimating the location of each node, it is possible to create a digital twin of the frame, as shown in Figure 16. This enables measurements of the displacement in both vertical and horizontal directions of each node of the frame at a given time, in comparison of the vertical displacement of the three dial gauges.

The central deflection is plotted in Figure 17, which shows good agreement between the measured data and the estimated data obtained using image recognition.

During the creep testing, the hangar experienced large variations in temperature, causing the steel beam connecting the two extremities to dilate and inducing undesirable vertical displacement in the gauge measurement. Fortunately, the temperature of the room was also recorded along with the gauge displacement, and the results were adjusted accordingly. However, the proposed method eliminates the dependence to temperature, making the measurement more stable.

4.2 MEMBER STRESS

By knowing the horizontal and vertical coordinates and the angle of rotation of each node at each step, it is possible to calculate the displacement and the rotation of each extremity of the member composing the lattice frame. Assuming that all the displacements occur in the 2D plane and using an initial Young's modulus, it is possible to apply the stiffness matrix and to calculate the axial force, shear force and bending moment of all the members. However, the current testing setup does not account for the displacement at the connection, and the results for vertical and diagonal members may differ significantly from reality. Additionally, the accuracy of angle measurement is questionable at this stage of research, so only the axial stress is calculated. Nevertheless, theoretically, it is possible to obtain all stresses of a member with this method with Equation (1) below:

$$\begin{bmatrix} a_N & 0 & 0 & -a_N & 0 & 0 \\ 0 & 12a_M & 6La_M & 0 & -12a_M & 6La_M \\ 0 & 6La_M & 4L^2a_M & 0 & -6La_M & 2L^2a_M \\ -a_N & 0 & 0 & a_N & 0 & 0 \\ 0 & -12a_M & -6La_M & 0 & 12a_M & -6La_M \\ 0 & 6La_M & 2L^2a_M & 0 & -6La_M & 4L^2a_M \end{bmatrix} \begin{Bmatrix} u_1 \\ v_1 \\ \theta_1 \\ u_2 \\ v_2 \\ \theta_2 \end{Bmatrix} = \begin{cases} N_1 \\ Q_1 \\ M_1 \\ N_2 \\ Q_2 \\ M_2 \end{cases}, \quad \begin{cases} a_N = \frac{EA}{L} \\ a_M = \frac{EI}{L^3} \end{cases} \quad (1)$$

where L = member length, A = cross-sectional area, I = cross-sectional second moment of inertia, E = Young's modulus, u = axial displacement, v = transversal displacement, θ = the rotation angle, N = axial force, Q = shear force and M = bending moment for both extremities.

An example of results is shown in Figure 18 with a comparison to the computational model. The stress

direction, i.e., tension or compression, shows rather good agreement. As for the intensity, good results are obtained for the centre and top part; however, close to the connection to the ground, result improvements are required. The main cause seems to be the picture distortion.

4.3 MEMBER CREEP

The overall creep of the frame is estimated with the central deflection. But not all the members of the frame participate equally to the creep amplification, and in the case of countermeasures to reduce the creep are required, knowing the members that suffer the most from creep can be very efficient. Indeed, by increasing the cross-section of such a member, it is possible to reduce the stress intensity and therefore to creep impact on the structure, allowing a cost-efficient design.

In Figure 19, the evolution of the length of several members from 30 minutes after the beginning of the testing to its end is shown. As an example, according to the recorded data, reinforcement of the member section between nodes 0-1 seems to be the best option to reduce the overall displacement, as this member has the largest change in length during the testing span.

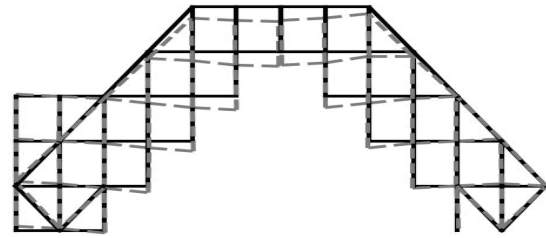


Figure 16: Original frame in black and estimated deformed frame in grey

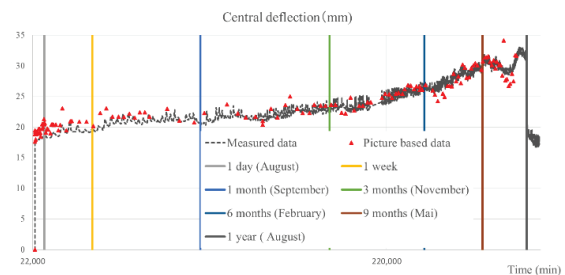


Figure 17: Comparison of the measured data and image recognition based estimations of the central deflection

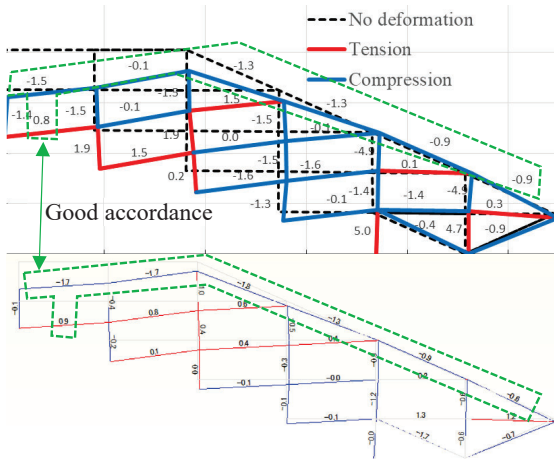


Figure 18: Stress intensity (in N/mm^2) comparison between the estimated model (top) and the computational model (bottom)

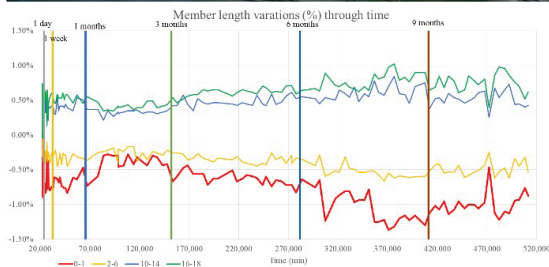
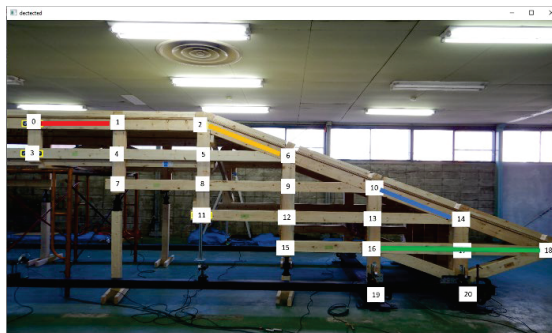


Figure 19: Top: Members layout, Bottom: Member length variations

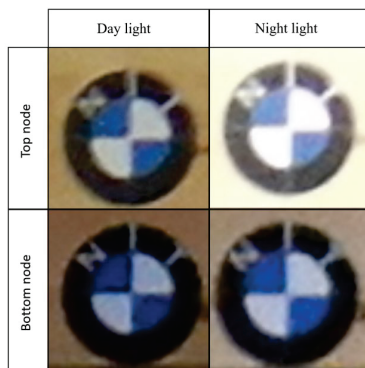


Figure 20: Comparison of 2 nodes during day and night time

5 LIMITATIONS AND IMPROVEMENT POINTS

5.1 TESTING SETUP

The testing setup was designed for standard creep testing and therefore was not optimized for the proposed method. For future developments, the following points should be revised.

5.1.1 Camera

The camera should be fixed on a weighted tripod to improve its stability. The camera should be actioned remotely to avoid any changes in distance or orientation relative to the frame and to avoid any blurring.

5.1.2 Environment

The lighting environment should be controlled to improve the continuity within a picture (space) and between the pictures (time), to reduce the disparities, as shown in Figure 20. Also, the camera should be set to manual to maintain the same aperture for all the pictures. The aperture should be around 8-12 to control lens aberration. A fixed low ISO is recommended to reduce the sensor noise.

5.1.3 Layout

The overlapping area of the cameras should be extended to improve the quality of the picture stitching. When better accuracy is required, the resolution and/or the number of cameras should be increased. In this testing, the resolution was about $70mm/55pixel$ or $1.3mm/pixel$.

5.1.4 Additional marking

Distinctive marks should be added at anchor points and close to them on the ground to create fix points. In this setup, the anchor points were connected by a steel beam, so the effect of the horizontal thrust and corresponding horizontal displacement was neglected. For structure with significant horizontal sliding, independent fix points are required.

5.1.5 References

To obtain precise results, a reference, such as a lead wire, should be added to set the vertical axis. Also a reference should be added to calculate the pixel/millimetre ratio to calibrate the lengths.

5.1.6 Template

A larger template should be used to calculate the rotation angle. With a 55×55 template, only rotation about 1 ($= \arctan(1/55)$) degree should be measurable. However, with the proposed image recognition procedure, subtle colour variations of the pixels are included, and a better resolution around 0.1 degree is obtained. The colours of the template should be selected to offer good contrast with timber or other testing material, and surrounding environment.

5.2 MULTILAYER STRUCTURE

The considered frame was composed of three layers. The marks were set only on the exterior layer, and therefore the displacement at the connection level due to the deformation of wood screws was not measurable. By adding additional marks close to the connection on the vertical member, as shown in Figure 21, the relative displacement between horizontal and vertical member at the connection can be estimated.

5.3 PROGRAMM

5.3.1 Step one and two: stitching and aligning

For the first step of the procedure, the picture stitching can be improved with the “SIFT” (Scale-Invariant Feature Transform) function from the OpenCV library. It locates key points on the both pictures and then compare them looking for similarities. It was tested for the available pictures of this test. However, the overlapping area was too small, with too large distortion and change in perspective, as shown in Figure 22. As a result, it was not possible to successfully apply it.

If enough trustable key points could be identified, the RANSAC (RANdom SAmple Consensus) algorithm could be applied to find a transformation (homography) that deforms continuously the first picture so that all its key points match those of the second picture.

This transformation process can also be applied to the second step to align and scale the pictures. However, only key points independent of the frame, i.e. which coordinates does not change over time, should be selected.

5.3.2 Step four: location and rotation

In the current procedure, the coordinates of the template mark are given in pixel, limiting the available precision. To improve this step, after the mark is located, a colour decomposition could be done to isolate the mark and identify its centre.

In this particular case of the presented testing, the mark is composed of blue, white and black. But, due to the lighting environment, white is sometimes considered as grey, and the blue/black mix is assimilated to violet in certain cases. Therefore, those two colours are also included in the allowed colour set for the mark isolation process. On the contrary, the wood colour is close to the yellow and red, and therefore, those two colours should be removed. The mark is obtained by adding the elements from the allowed colour set and subtracting the yellow and the red. A thresholding process is used to obtain a binary representation of the picture with the pixels of the mark in white and the other pixels in black, as shown in Figure 23. Then the “findContours” function from the OpenCV library is applied to identify the mark outer shape and estimate its centre with better precision. The mark is approximated by an ellipse, so that the length difference of the major and minor axis and their rotation angle can also be used to reduce distortion.

In addition, this method can also be used to locate accurately the straight lines of the mark and identify directly its rotation angle. The procedure should be faster, but resolution is likely to be worsen. An appropriate choice is needed according to the application.

5.3.3 Distortion

In the end, the most important improvement should be to add an algorithm to reduce or cancel the distortion from the lens and perspective, so that the proportions, parallel lines, and perpendicular lines are preserved.

Calibration of the camera using chessboard could be done along with other calibration depending on the layout of the testing setup.

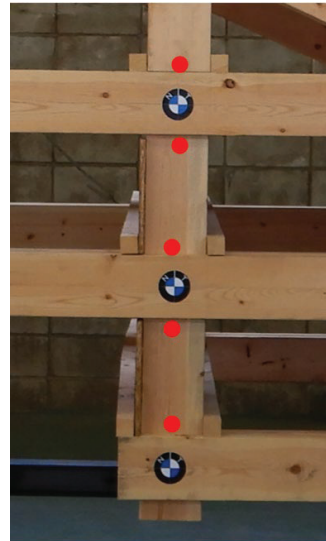


Figure 21: Example of additional marks to estimate inner layer displacement. Rotation is not required, therefore simple mark is enough.

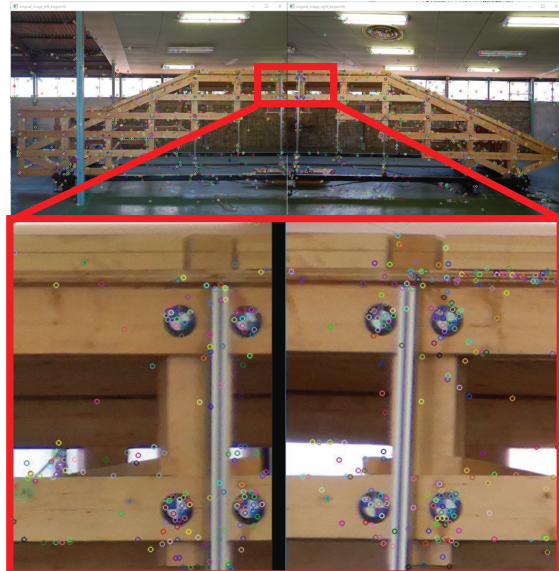


Figure 22: Key points comparison for left and right picture

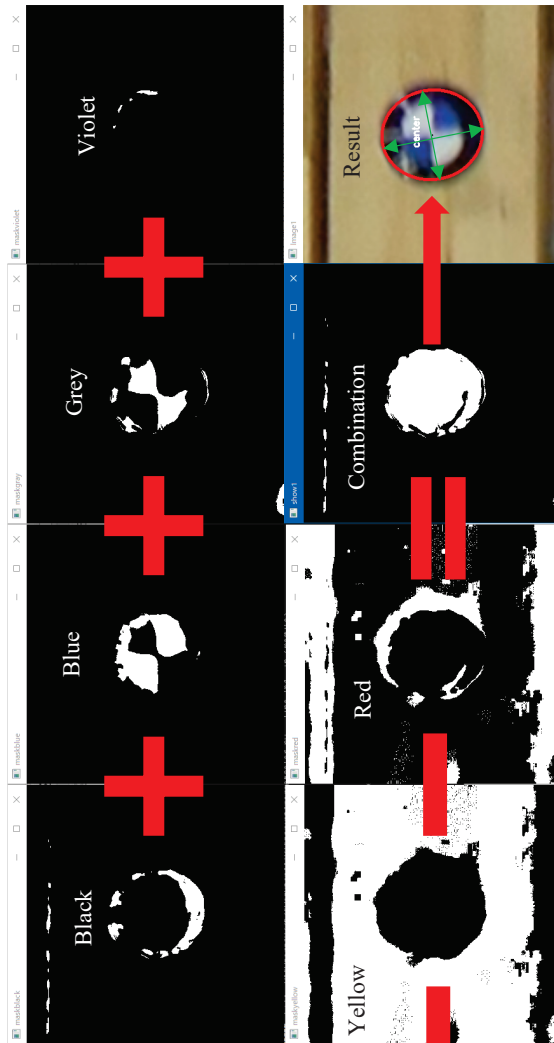


Figure 23: Colour decomposition with black and with thresholding followed by a combination to isolate the mark contour and identify its centre

6 CONCLUSIONS

In conclusion, the proposed method of using image processing and analysis techniques for measuring the deformation of timber structures has shown promising results.

However, there are limitations and improvement points that need to be addressed to increase the accuracy and reliability of the method. These include optimizing the testing setup, improving the stitching and aligning of the images, and reducing distortion from the lens and perspective. By addressing these issues, the proposed method has the potential to provide a cost-effective, non-destructive and precise means of measuring the deformation, stress of timber structures among other, which can have important applications in the field of civil engineering and architecture.

Further research and development in this area can lead to more accurate and efficient methods for monitoring the structural integrity of timber buildings and bridges, ultimately contributing to safer and more sustainable infrastructure.

REFERENCES

- [1] S. M. Holzer, J. R. Loferski, and D. A. Dillard: A review of creep in wood: concepts relevant to develop long-term behavior predictions for wood structures. In: *Wood and Fiber Science*, 21(4), pp. 376-392, 1989.
- [2] N. Giron, N. Nakanishi, K. Matsuo, R. Arai and H. Nasu: Lattice framed roof formed of superimposed lumber and joined by wood screws and LVL gussets. In: *WCTE2021*, 2027-2035, 2021.